Equal Channel Angular Extrued $Bi_{0.5}Sb_{1.5}Te_3$ Thermoelectric Compound

CheolHo Lim[1]*, KyungTaek Kim[2], YongHwan Kim[2], ChangHun Lee[1,]* and ChiHwan Lee[1]

[1]*Dept. of Metallurgical Engineering, College of Engineering, Inha University,
253 Yonghyun-Dong, Nam-Gu, Incheon, 402-751, Korea*
[2]*New Functional Materials Team, Korea Institute of Industrial Technology,
7-47 Songdo-Dong, Yeonsu-Gu, Incheon, 406-840, Korea*

The effects of equal channel angular extrusion (ECAE) process parameters on microstructure and thermoelectric properties of the p-type $Bi_{0.5}Sb_{1.5}Te_3$ compound have been investigated. ECAE was carried out under various temperatures (653 K, 693 K, 733 K) and ram speeds (0.5 mm/s, 1 mm/s, 2 mm/s). Fraction of recrystallized grains and grain size was found to be increase with lower ram speed and higher deformation temperature. As a result, Seebeck coefficient increased, and electrical resistivity and thermal conductivity decreased. The decrease in thermal conductivity was attributed to the decrease of lattice thermal conductivity (κ_{ph}) which is independent of electrical properties. Maximum figure-of-merit (2.87×10^{-3} K^{-1}) was achieved in as-ECAE'ed specimen at 733 K and at ram speed of 0.5 mm/s. This value was found to be 6% higher than that of as-sintered specimen. [doi:10.2320/matertrans.MEP2007297]

1. Introduction

Single crystal and unidirectionally solidified Bi_2Te_3-based compounds are widely used as low temperature thermoelectric materials because their thermoelectric properties are excellent at the temperature range of 200∼400 K. This compound is easily fractured along the basal plane of the hexagonal layered structure because $Te^{(1)}$-$Te^{(1)}$ plane is weakly bound with van der Waals force.[1] Thus, powder metallurgy has been developed to obtain enhanced mechanical properties of Bi_2Te_3-based compound. Bending strength of sintered compounds fabricated by the technique such as hot extrusion and spark plasma sintering shows 3∼5 times higher value compared with that of single crystal.[2,3] However, it has a weakness that figure-of-merit for Bi_2Te_3-based compounds prepared by powder metallurgy lower than single crystal due to oxidation, contamination, and lowered orientation.

One of the solutions to improve performance of polycrystalline thermoelectric material is to reduce thermal conductivity through grain refinement.[4,5] Recently, ECAE process which is the heavy plastic deformation method was applied to bulk thermoelectric material.[6–8] This technique can accumulate strain in the work piece because during the process the specimen is severe plastically deformed without reduction of cross sectional size. Therefore, the ECAE process is effective in grain refinement of bulk materials than any other processes, and more favorable to reduce grain size under the condition of relatively low temperature and high strain rate.

In the present study, ECAE process was applied for microstructure control of sintered p-type $Bi_{0.5}Sb_{1.5}Te_3$ compound in order to enhance thermoelectric properties. From the microstructure evolution via ECAE process parameters including deformation temperature and ram speed, we investigated in detail for thermoelectric properties such as Seebeck coefficient, electrical resistivity, and thermal conductivity.

2. Experimental Procedures

High purity elements (Bi, Te, Sb) were put into a quartz tube, which was vacuum-sealed at 1.33×10^{-3} Pa. The mixtures were melted at 1023 K for 2 hours by using a rocking furnace to ensure homogeneity of the composition. The solidified ingots were crushed into flakes under N$_2$ atmosphere and then sieved to 45∼105 μm. The obtained powders were reduced at 653 K for 10 hours in hydrogen to remove oxygen absorbed during crushing. P-type 2 mass% Te-doped $Bi_{0.5}Sb_{1.5}Te_3$ sintered by spark plasma sintering system (Dr. Sinter 1050) at 653 K for 4 minutes.

The sintered specimens ($\phi = 8$ mm, $h = 40$ mm) were equal channel angular extruded at the various ram speeds (0.5 mm/s, 1 mm/s, 2 mm/s) and deformation temperatures (653 K, 693 K, 733 K). Here, the ram speed means moving speed of plunger applying pressure to the specimen. Also, ECAE'ed specimen was quenched in water to avoid grain growth. The die for ECAE was made of SKD61 tool steel with an internal angle (Φ) of 90° and an outer curvature spanning (Ψ) of 20°.

The thermoelectric properties were conducted at room temperature. The Seebeck coefficient α was determined by using $\alpha = \Delta V/\Delta T$ with imposed temperature difference of 10 K at both ends of the specimen. The electrical resistivity ρ was measured by the four-probe technique using sourcemeter(Keithley 2400) and nanovolt-meter(Keithley 2182). The thermal conductivity κ was measured by the static comparative method using transparent SiO$_2$ ($\kappa = 1.36$ W/mK at room temperature) as a standard sample in 6.65×10^{-3} Pa.

3. Results and Discussion

For ECAE, sintered p-type $Bi_{0.5}Sb_{1.5}Te_3$ compound was prepared by spark plasma sintering method and then inserted into a copper-aluminum twofold can to avoid fracture of compound during process. Figure 1 shows the sintered compound and as-ECAE'ed specimen. As identified in cross section of as-ECAE'ed specimen, the $Bi_{0.5}Sb_{1.5}Te_3$ com-
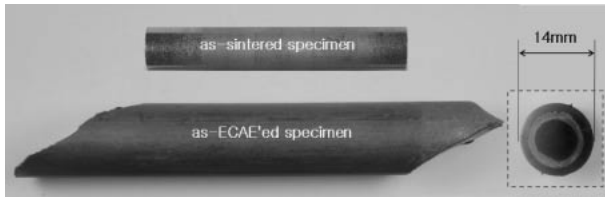
---

*Graduate Student, Inha University

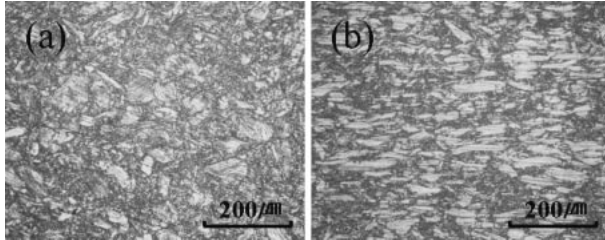Fig. 1 Photographs of spark plasma sintered and as-ECAE'ed specimen.

Fig. 2 Optical micrographs of spark plasma sintered specimen observed (a) in the perpendicular section and (b) in the parallel section to the pressing direction.
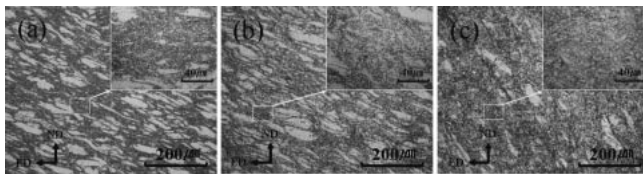

Fig. 3 Optical micrographs of as-ECAE'ed specimens deformed at various deformation temperatures with ram speed of 1 mm/s (ED: extrusion direction, ND: normal direction); (a) 653 K, (b) 693 K, (c) 733 K.
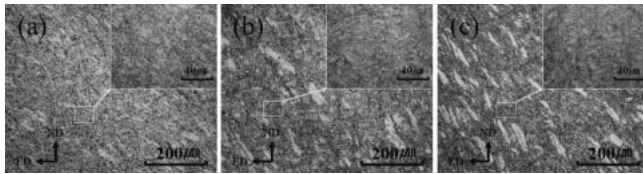

Fig. 4 Optical micrographs of as-ECAE'ed specimens deformed with various ram speeds at 733 K; (a) 0.5 mm/s, (b) 1 mm/s, (c) 2 mm/s.

pound was successfully deformed without fracture.

Figure 2 shows microstructure of the sintered compound. Most of grains were not recrystallized and maintained initial particle size (45~105 μm) due to low strain although 653 K was high sintering temperature enough for recrystallizing the $Bi_{0.5}Sb_{1.5}Te_3$ compound. At the perpendicular section to the pressing direction grains shows the shape of abnormal grain with various sizes, and at the parallel section to the pressing direction grains is lined up to the same direction.

Figure 3 and 4 show effect of deformation temperature and ram speed on microstructures of the $Bi_{0.5}Sb_{1.5}Te_3$ compound after single pass. Figure 3 is micrographs of specimen deformed at different deformation temperatures (653 K, 693 K, 733 K) with ram speed of 1 mm/s, which observed in transverse section. The as-ECAE'ed specimen at 653 K mainly consists of large grain with initial particle size and unrefined grain was found to be rotated about 30° clockwise
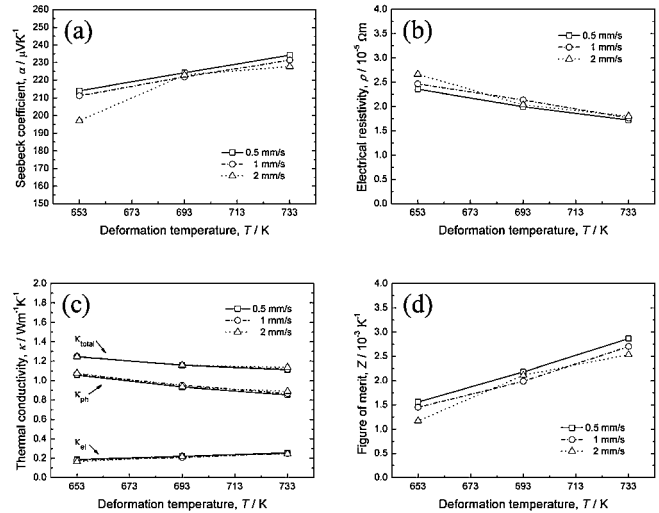

Fig. 5 Thermoelectric properties of as-ECAE'ed sepecimens deformed at various deformation temperatures under ram speed of 0.5 mm/s, 1 mm/s, and 2 mm/s; (a) Seebeck coefficient, (b) Electrical resistivity, (c) Thermal conductivity, (d) Figure-of-merit.

from the initial position. As shown in the enlarged micrograph of Fig. 3, refined grains were locally observed between unrecrystallized large grains and exhibited equiaxed microstructure with 1~3 μm size. As deformation temperature was increased, fraction of recrystallized grains increased and the refined grain grew up to 6~12 μm at 733 K. Figure 4 illustrated the micrographs of specimen deformed at different ram speeds (0.5 mm/s, 1 mm/s, 2 mm/s) at 733 K, which is observed at transverse section. Fraction of recrystallized grains increased as ram speed is slow. Consequently, specimen deformed at ram speed of 0.5 mm/s was almost recrystallized.

To investigate the effect of microstructural changes by recrystallization on thermoelectric properties, Seebeck coefficient, electrical resistivity, and thermal conductivity was measured at room temperature, and figure-of-merit ($Z = \alpha^2/\rho \cdot \kappa$) was calculated from the results. Thermoelectric properties of spark plasma sintered specimen before ECAE were summarized in Table 1. Figure 5(a) shows Seebeck coefficient with various deformation temperatures and ram speeds. Seebeck coefficient tends to increase as deformation temperature increases and ram speed decreases. From Boltzmann distribution, Seebeck coefficient α of thermoelectric material can be expressed by eq. (1).[9]

$$\alpha = \pm \frac{k_B}{e}[r - \ln n_c + c] \tag{1}$$

Here, k_B is Boltzmann constant, e is the electronic charge, m^* is effective mass, n_c is carrier concentration. Scattering factor r is 0 for scattering mode by lattice vibration. Thus it is considered that the increase of Seebeck coefficient is due to the decrease of carrier concentration.

It is known that $(Bi,Sb)_2Te_3$ compound forms the defect as shown in eqs. (2) and (3) because tellurium having high vapor pressure is vaporized easily during the casting.[10]
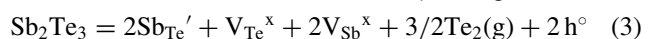
$$Bi_2Te_3 = 2Bi_{Te}' + V_{Te}^x + 2V_{Bi}^x + 3/2Te_2(g) + 2h° \tag{2}$$
$$Sb_2Te_3 = 2Sb_{Te}' + V_{Te}^x + 2V_{Sb}^x + 3/2Te_2(g) + 2h° \tag{3}$$

Table 1 Thermoelectric properties of spark plasma sintered specimen.

Seebeck coefficient	Thermal conductivity			Electrical resistivity	Figure-of-merit
	κ_{total}	κ_{ph}	κ_{el}		
$217\,\mu m\,K^{-1}$	$1.25\,W\,m^{-1}\,K^{-1}$	$0.32\,W\,m^{-1}\,K^{-1}$	$0.93\,W\,m^{-1}\,K^{-1}$	$1.38 \times 10^{-5}\,\Omega m$	$2.72 \times 10^{-3}\,K^{-1}$

Park et al.[11] reported that Te interstitial which was generated by plastic deformation occupy Bi vacancy or Sb vacancy sites which already existed in lattice as shown in eqs. (2) and (3), thus generating an excess free electron as follow.

$$Te_i^x + V_{Bi}^x(\text{or } V_{Sb}^x) \rightarrow Te_{Bi}(\text{or } Te_{Sb}) + e' \qquad (4)$$
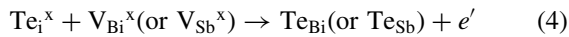
In addition, Schultz et al.[12,13] reported that nonbasal slip by heavy plastic deformation produces plentiful Te vacancy-interstitial pairs (Frenkel defects) in Bi_2Te_3 compound and Te vacancy which is electrically active plays a role as a donor. In conclusion, it is considered that the increase of Seebeck coefficient was attributed to the increase of electron by plastic deformation. Because of these reasons, Seebeck coefficient ($180\,\mu m/K$) of ingot increased to $217\,\mu m/K$ after sintering and Seebeck coefficient of as-ECAE'ed specimen more increased as deformation temperature increased.

Figure 5(b) shows electrical resistivity with various deformation temperatures and ram speeds. Electrical resistivity tends to decrease as deformation temperature become higher and ram speed become lower. Electrical resistivity is inversely proportional to carrier concentration and mobility. Thus, it is considered that electrical resistivity decreased because carrier mobility is significantly improved as deformation temperature become higher and ram speed become lower despite the decrease in carrier concentration. The improvement in carrier mobility is considered to be attributed to reduction of grain boundary scattering by grain growth and lattice stress relaxation by recovery.

Figure 5(c) shows thermal conductivity with various deformation temperatures and ram speeds. Thermal conductivity was not strongly affected by ram speed, but shows a tendency to decrease as deformation temperature increase. For metal, thermal conduction by electron mostly contributes to entire thermal conduction. However, for semiconductor, thermal conduction by lattice vibration (or phonon) as well as by electron also contributes to entire thermal conduction. It is known that electronic thermal conductivity κ_{el} is about $1/3\sim1/4$ to lattice thermal conductivity κ_{ph} in Bi_2Te_3 based thermoelectric material.[14,15] Electronic thermal conductivity κ_{el} and lattice thermal conductivity κ_{ph} calculated from Wiedemann-Franz law was shown in Fig. 5(c). It is apparent that the variation of thermal conductivity is mainly attributed to lattice thermal conductivity κ_{ph}. At low temperature and high ram speed, lattice thermal conductivity shows relatively high value because recrystallized grain size is very fine but lots of unrecrystallized grain exists in matrix.

Figure 5(d) shows figure-of-merit calculated from Seebeck coefficient, electrical resistivity, and thermal conductivity. As deformation temperature increases and ram speed decrease figure-of-merit is improved. This result is attributed to the increase of Seebeck coefficient and the decrease of electrical resistivity and thermal conductivity. The maximum figure-of-merit is $2.87 \times 10^{-3}\,K^{-1}$ for the specimen deformed at 733 K at 0.5 mm/s.

4. Conclusion

The effect of deformation temperature and ram speed on microstructure and thermoelectric properties of sintered p-type $Bi_{0.5}Sb_{1.5}Te_3$ compound have been investigated through ECAE process. As deformation temperature increases and ram speed decreases dynamic recrystallization was effectively occurred. Consequently, the specimen deformed at 733 K under the ram speed of 0.5 mm/s was fully recrystallized. Under the low deformation temperature and high ram speed, a size of recrystallized grain was more refined, whereas fraction of recrystallized grains was reduced. Figure-of-merit tended to be strongly affected by fraction of recrystallized grains and showed maximum value at deformation temperature of 733 K and at ram speed of 0.5 mm/s. Also, this value is 6% higher than that of sintered specimen, resulting from that Seebeck coefficient increases and thermal conductivity decreases after ECAE. It is considered that the decrease of thermal conductivity was attributed to the decrease of lattice thermal conductivity (κ_{ph}) due to the grain refinement by dynamic recrystallization.

REFERENCES

1) J. R. Weise and L. Muller: J. Phys. Chem. Solids **15** (1960) 13.
2) J. Seo, D. Lee, C. Lee and K. Park: J. Mater. Sci. Lett. **16** (1997) 1153.
3) D. M. Lee, C. H. Lim, S. Y. Shin, D. C. Cho and C. H. Lee: J. Electroceram. **17** (2006) 879.
4) D. H. Kim and T. Mitani: J. Alloy Compd. **399** (2005) 14.
5) A. A. Joraide: J. Mater. Sci. **30** (1995) 744.
6) J. T. Im, K. T. Hartwig and J. Sharp: Acta Mater. **52** (2004) 49.
7) S. S. Kim, S. Yamamoto and T. Aizawq: J. Alloy Compd. **375** (2004) 107.
8) X. A. Fan, J. Y. Yang, W. Zhu, S. Q. Bao, X. K. Duan, C. J. Xiao and K. Li: J. Alloy Compd. (2007), (doi:10.1016/j.jallcom.2007.07.007).
9) J. Seo, K. Park, D. Lee and C. Lee: Scripta Mater. **38** (1998) 477.
10) Z. Stary, J. Horak, M. Stordeur and M. Stolzer: J. Phys. Chem. Solids **49** (1988) 29.
11) T. H. Park, H. I. Yoo and J. D. Shim: J. Kor. Ceram. Soc. **29** (1992) 885.
12) J. M. Schultz, J. P. Mchugh and W. A. Teller: J. Appl. Phys. **33** (1962) 2443.
13) P. Delavignette and S. Amelinckx: Philos. Mag. **5** (1960) 729.
14) D. A. Wright: Metallurgical Rev. **15** (1970) 147.
15) F. D. Rosi: Solid State Electron. **11** (1968) 833.